

Received 7 April 2026

Accepted 25 April 2026

Edited by W. T. A. Harrison, University of  
Aberdeen, United Kingdom**Keywords:** crystal structure; phenanthroline-5,6-  
dione derivative; O—H...N and C—H...O  
hydrogen bonds; Hirshfeld surface analysis.**CCDC reference:** 2549869**Supporting information:** this article has  
supporting information at journals.iucr.org/e

# Synthesis and structure of (*RS*)-6-hydroxy-6-(2-oxopropyl)-1,10-phenanthroline-5(6*H*)-one

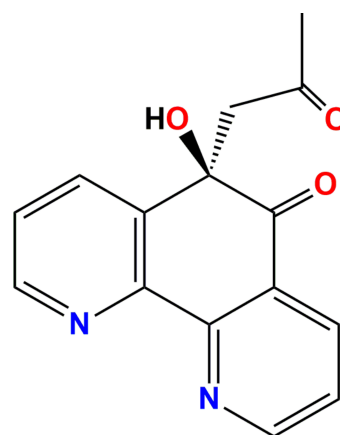
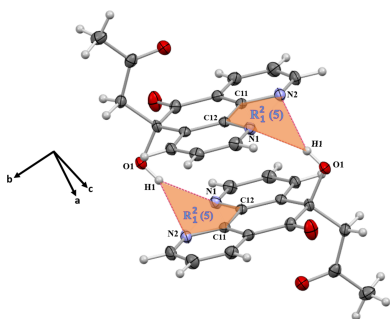
Tarek Benlatreche,<sup>a,b\*</sup> Abderrahmane Mezrag,<sup>c,d</sup> Boutheina Boualia<sup>a</sup> and Stéphane Golhen<sup>e</sup>

<sup>a</sup>Environmental and Structural Molecular Chemistry Research Unit, URCEMHS, Faculty of Exact Sciences, University of Constantine 1-Mentouri Brothers, 25000, Algeria, <sup>b</sup>National Higher School for Hydraulics, Abdellah Arbaoui, Blida, Algeria, <sup>c</sup>Research Unit Development of Natural Resources, Bioactive Molecules and Physiochemical and Biological Analysis, Department of Chemistry, Constantine 1 University, Constantine 25000, Algeria, <sup>d</sup>Faculty of Science, Department of Organic Chemistry, Saad Dahleb University, Blida 1, Algeria, and <sup>e</sup>CNRS, Rennes Institute of Chemical Sciences -UMR 6226, University of Rennes, France. \*Correspondence e-mail: benlatreche.tarek.33@gmail.com

The title compound, C<sub>15</sub>H<sub>12</sub>N<sub>2</sub>O<sub>3</sub>, was synthesized by reacting phendione with acetone in ethanol under microwave irradiation. An intramolecular C=O... $\pi$  interaction supports the molecular conformation. In the crystal, inversion dimers linked by pairwise, bifurcated O—H... $(N,N)$  hydrogen bonds are seen and the dimers are further linked by weak C—H...N and C—H...O hydrogen bonds and aromatic  $\pi$ – $\pi$  stacking interactions. Hirshfeld surface analysis shows the following contact percentages: H...H 36.8%; H...O/O...H 26.1%; H...C/C...H 14.9%; H...N/N...H 14.5%; C...C 5.3%, with all other contact types making negligible contributions.

## 1. Chemical context

1,10-Phenanthroline-5,6-dione (phendione, C<sub>12</sub>H<sub>6</sub>N<sub>2</sub>O<sub>2</sub>) is a quinonoid derivative of 1,10-phenanthroline, characterized by the presence of two carbonyl groups at positions 5 and 6 of the aromatic core, which confers both diimine- and quinone-type reactive sites. This dual functionality provides significant versatility in coordination chemistry, allowing it to bind to metal ions primarily through the nitrogen atoms of the diimine moiety (Ermakova *et al.*, 2023), while in certain cases also engaging the oxygen atoms of the carbonyl groups in the coordination process (Jing *et al.*, 2011).



Phendione and its derivatives have broad applications in biology (Pivetta *et al.*, 2014; McCann *et al.*, 2012), chemistry, and medicinal chemistry. Their complexes, particularly those formed with Cu<sup>II</sup> and Ag<sup>I</sup>, exhibit antimicrobial (Galdino *et al.*, 2022), antifungal (Granato *et al.*, 2017) and antitumor

activities (Deegan *et al.*, 2006) due to their ability to interact with DNA and disrupt cellular redox processes (Pivetta *et al.*, 2014). They thus target both cancer cells and drug-resistant bacteria, making them promising candidates for the development of new therapeutic agents (Granato *et al.*, 2021).

As part of our studies in this area, we now describe the synthesis and structure of the title compound, C<sub>15</sub>H<sub>12</sub>N<sub>2</sub>O<sub>3</sub> (**I**). We are particularly interested in this molecule because of its promising biological properties observed in our previous investigations, especially its anticholinesterase and antifungal activities against several tested strains. In addition, this compound exhibits a strong ability to coordinate with metal ions due to the presence of suitable donor atoms in its structure. In our work, special attention is given to its interaction with tin, as organotin derivatives are known to exhibit enhanced biological activities. Therefore, the synthesis and characterization of such complexes are of particular interest, not only to evaluate their potential biological properties, but also to gain deeper insight into the structure–activity relationships. This approach is fully consistent with our research objectives, which focus on the development of new bioactive compounds through coordination chemistry.

## 2. Structural commentary

Compound (**I**) crystallizes in the monoclinic space group *P*<sub>2</sub><sub>1</sub>/*c* with one molecule in the asymmetric unit (Fig. 1). The acetone moiety is attached to the aromatic core *via* atom C13 and adopts an approximately planar conformation, as indicated by the O3–C14–C13–C5 torsion angle of –11.3° (2), which may be associated with an intramolecular C14=O3··· $\pi$  interaction with O···C<sub>g</sub> = 2.7130 (16) Å and C=O··· $\pi$  = 98.71 (11)°. The dihedral angle between the acetone group and the phenanthroline ring system is 84.99 (5)°, reflecting an almost perpendicular orientation. Bond lengths in the molecule vary from 1.211 (2) Å (O3–C14) to 1.545 (3) Å (C5–C6), while bond angles range from 107.86 (14)°

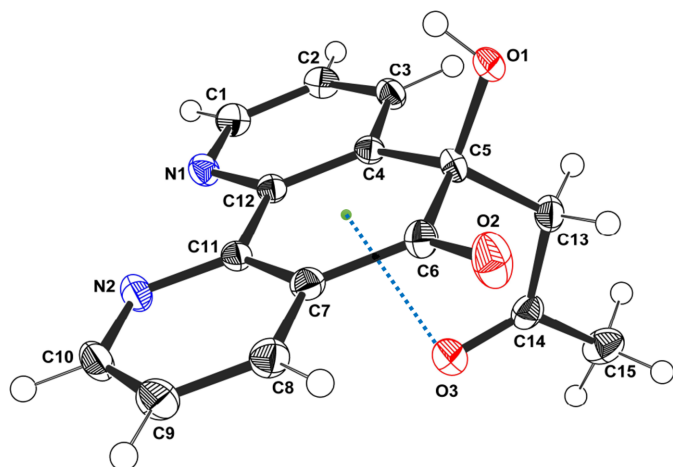


**Figure 1**  
The asymmetric unit of (**I**) with displacement ellipsoids drawn at the 50% probability level.

**Table 1**  
Hydrogen-bond geometry (Å, °).

<i>D</i> –H··· <i>A</i>	<i>D</i> –H	H··· <i>A</i>	<i>D</i> ··· <i>A</i>	<i>D</i> –H··· <i>A</i>
O1–H1···N1 <sup>i</sup>	0.84	2.22	2.977 (2)	149
O1–H1···N2 <sup>i</sup>	0.84	2.56	3.262 (2)	142
C13–H13A···O1 <sup>ii</sup>	0.99	2.52	3.457 (2)	158
C15–H15B···O1 <sup>ii</sup>	0.98	2.67	3.561 (3)	152
C1–H1A···O1 <sup>iii</sup>	0.95	2.63	3.302 (2)	128
C3–H3···N1 <sup>iii</sup>	0.95	2.83	3.727 (2)	158
C8–H8···O2 <sup>iv</sup>	0.95	2.62	3.436 (3)	145
C10–H10···O3 <sup>v</sup>	0.95	2.59	3.235 (2)	125
C15–H15A···O3 <sup>vi</sup>	0.98	2.69	3.254 (3)	117

Symmetry codes: (i)  $-x + 1, -y + 1, -z$ ; (ii)  $x, -y + \frac{1}{2}, z + \frac{1}{2}$ ; (iii)  $-x + 1, y + \frac{1}{2}, -z + \frac{1}{2}$ ; (iv)  $-x + 2, -y + 1, -z$ ; (v)  $x, -y + \frac{3}{2}, z - \frac{1}{2}$ ; (vi)  $-x + 2, -y + 1, -z + 1$ .

(O1–C5–C6) to 124.13 (18)° (N2–C10–C9). The molecule features a quasi-planar aromatic core, whereas the carbonyl groups and peripheral substituents adopt moderate distortions to reduce steric interactions, as illustrated by the torsion angles C3–C4–C5–O1 = 58.65 (19)°, C3–C4–C5–C13 = –57.3 (2)°, C12–C4–C5–O1 = –118.38 (16)° and C12–C4–C5–C13 = 125.62 (17)°. Atom C5 is a stereogenic (chiral) centre: in the arbitrarily-chosen asymmetric unit, it has *R* configuration, but crystal symmetry generates a racemic mixture.

## 3. Supramolecular features

In the extended structure of (**I**), an asymmetric, bifurcated O1–H1···(N1,N2) interaction, with H···*A* distances of 2.22 and 2.56 Å, respectively (sum of angles at H1 = 359°), gives rise to an *R*<sub>1</sub><sup>2</sup>(5) ring motif, linking the molecules into inversion dimers (Table 1, Fig. 2). The hydrogen bonds C13–H13A···O1 and C15–H15B···O1, with H···*A* distances of 2.52 and 2.67 Å, respectively, generate *R*<sub>2</sub><sup>1</sup>(6) loops connecting adjacent molecules, which propagate along the *c*-axis direction (Fig. 3). Two *R*<sub>2</sub><sup>2</sup>(8) motifs are also observed: the first is formed by C1–H1A···O1 and

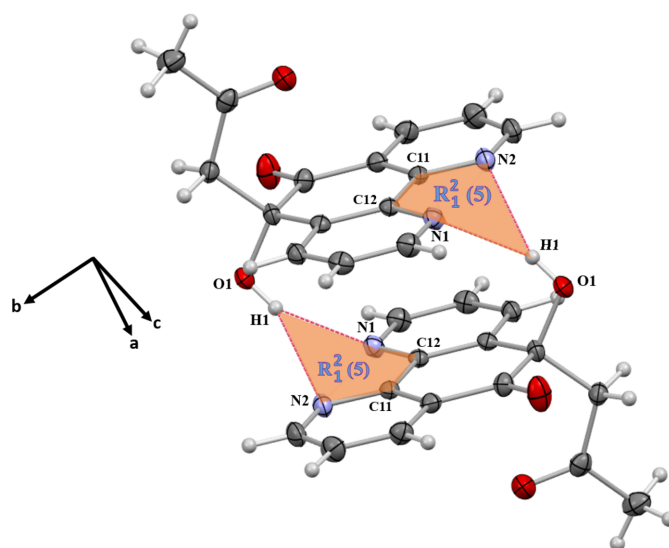


**Figure 2**  
Detail of the packing of (**I**) illustrating the bifurcated O1–H1···(N1,N2) hydrogen bonds, which form an inversion dimer.

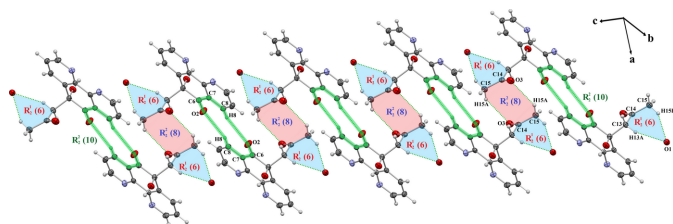


**Figure 3**  
Detail of the packing of (**I**) showing the C15–H15B···O1, C13–H13A···O1, C15–H15A···O3 and C8–H8···O2 hydrogen bonds, forming different ring motifs.

C3–H3···N1 ( $H\cdots A = 2.63$  and  $2.83$  Å; Fig. 4), while the second arises from C15–H15A···O3 ( $H\cdots A = 2.69$  Å; Fig. 3). These motifs repeat along the *b* and *c* axes, respectively, contributing to the long-range organization of the crystal. The C8–H8···O2 interaction ( $H\cdots A = 2.62$  Å) forms an  $R_2^2(10)$  ring motif linking two neighboring molecules, propagating along the *c*-axis direction (Fig. 3). Additionally, the C3–H3···N1 bond generates  $C(5)$  chains extending parallel to the *b*-axis direction (Fig. 4), further reinforcing the continuity of hydrogen-bonding interactions within the structure.

The three-dimensional architecture is consolidated by aromatic  $\pi$ – $\pi$  stacking interactions between superposed molecules. The centroid–centroid distances are 3.6098 (12) and 3.4902 (11) Å, observed between the ring centroids Cg1 and Cg2' [symmetry code: (')  $1 - x, 1 - y, -z$ ], where Cg1 and Cg2 correspond to the N1/C1–C4/C12 and N2/C7–C10/C11 rings, respectively, as well as Cg1 and Cg3', where Cg3 represents the centroid of the C11/C4–C7/C12 ring (Fig. 5).

#### 4. Database survey

A search of the Cambridge Structural Database (CSD, version 2025.3.1, update of February 2026; Groom *et al.*, 2016) for compounds similar to (**I**) was undertaken.

Database analysis revealed that the structure of (**I**) had not been reported previously, although similar structures were identified in monoatomic ruthenium(II), copper(II), and tin(IV) complexes. These structures, with CSD refcodes ATOPUU (Fujihara *et al.*, 2004), RUZQEJ (Karnahl *et al.*, 2010) and TILQOY (Benlatreche, 2023), crystallize in space groups  $C2/c$ ,  $P\bar{1}$  and  $Pna2_1$ , respectively. Furthermore, another ligand, formed in a distinct complex (JIVPOX; Golubeva *et*

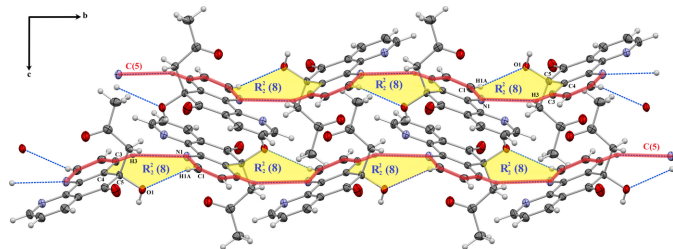


**Figure 4**  
Crystal packing of (**I**) illustrating the C1–H1A···O1 and C3–H3···N1 hydrogen bonds forming a ring motif; and  $C(5)$  chains extending parallel to the *b*-axis direction, respectively.

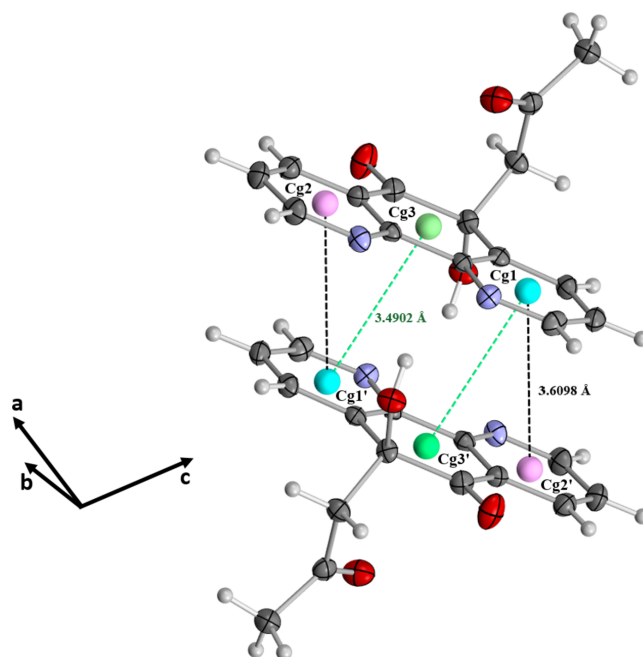


**Figure 5**  
Depiction of  $\pi$ – $\pi$  stacking interactions between the aromatic rings of superposed molecules, with centroid–centroid distances (Cg1···Cg2'/Cg1···Cg3') highlighted.

*al.*, 2023), exhibits a structure similar to our molecule, with the difference that the acetone group is replaced by an ethoxy group. This complex crystallizes in space group  $P\bar{1}$ .

#### 5. Hirshfeld surface analysis

In order to further quantify the intermolecular interactions contributing to the organization of the crystal packing, a Hirshfeld surface (HS) analysis, accompanied by an analysis of the associated two-dimensional fingerprint plots (FP), was carried out using *CrystalExplorer 21.5* (Spackman *et al.*, 2021).

The Hirshfeld  $d_{\text{norm}}$  surfaces were mapped over the range  $-0.41$  to  $1.36$  Å using a fixed colour scale from 0.76 (red) to 2.4 (blue). The Hirshfeld surface was further investigated through the associated two-dimensional fingerprint plots, which provide a quantitative representation of the intermolecular contacts within the crystal structure. As shown in Fig. 6*a*,  $H\cdots H$  contacts constitute the major contribution to the Hirshfeld surface, accounting for 36.8% of the total surface area. These contacts mainly arise from  $C-H\cdots H$  interactions and emphasize the predominance of van der Waals forces in the crystal packing. The  $O\cdots H/H\cdots O$  contacts, shown in Fig. 6*b*, correspond to  $C-H\cdots O$  hydrogen-bond interactions and represent the second most important contribution, accounting for 26.1% of the total interactions.

Fig. 6*c* displays the  $H\cdots C/C\cdots H$  contacts, which are associated with  $C-H\cdots \pi$  interactions and contribute 14.9% to the Hirshfeld surface. In addition, the  $N\cdots H/H\cdots N$  contacts (Fig. 6*d*), attributable to  $O-H\cdots N$  hydrogen bonds, represent 14.5% of the total surface area, highlighting the role of these interactions in the supramolecular assembly. The  $C\cdots C$

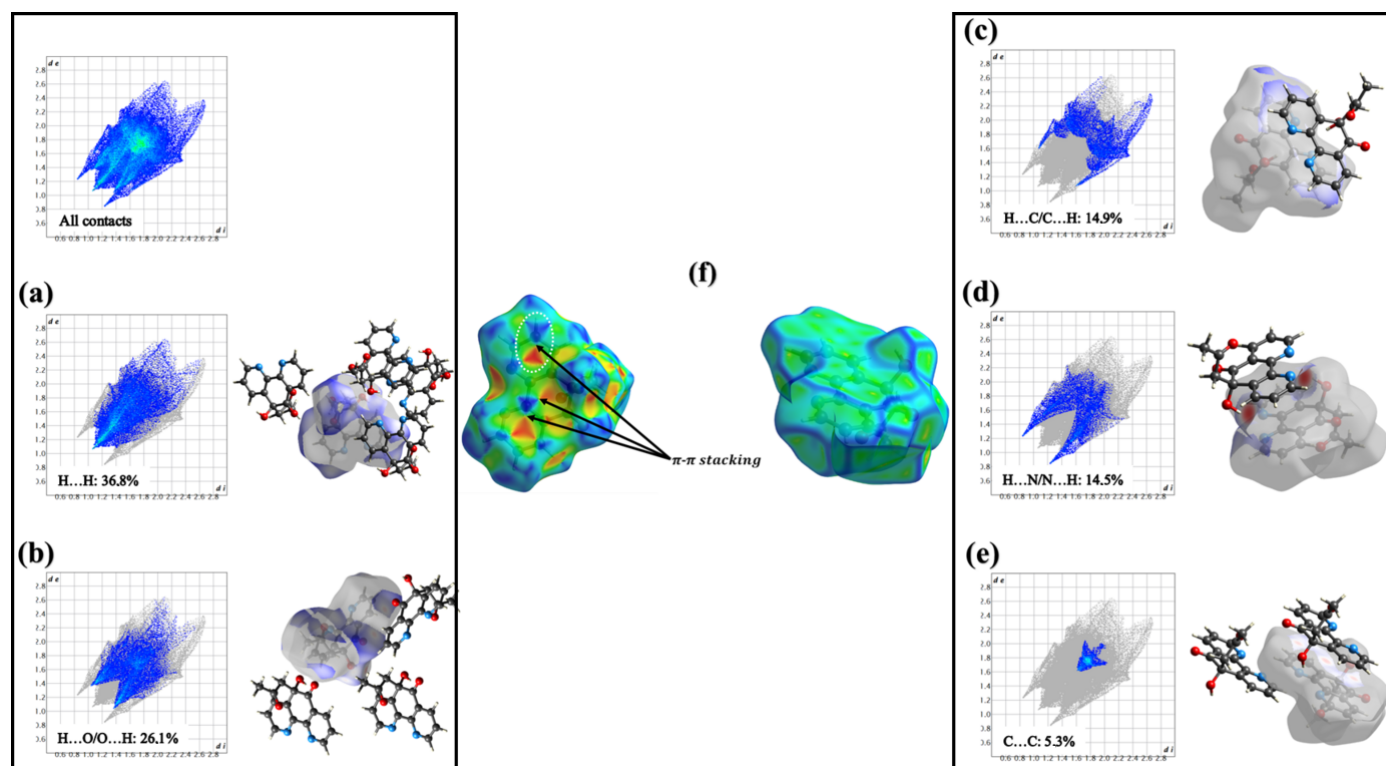


**Figure 6**  
Hirshfeld surface analysis and two-dimensional fingerprint plots of the title compound illustrating: (a) H...H contacts, (b) O...H/H...O contacts, (c) H...C/C...H contacts, (d) N...H/H...N contacts, (e) C...C contacts; and Hirshfeld surface representations of the (f) shape-index and curvedness, highlighting  $\pi$ - $\pi$  stacking interactions.

contacts illustrated in Fig. 6e account for 5.3% of the total interactions and are indicative of  $\pi$ - $\pi$  stacking interactions between aromatic rings (Fig. 6f). Other intermolecular contacts appear only as minor contributions in the fingerprint plots, including N...C/C...N (1.7%), O...C/C...O (0.5%) and O...O (0.2%) contacts.

## 6. Synthesis and crystallization

In a 10 ml glass vial, 0.25 mmol of 1,10-phenanthroline-5,6-dione was combined with an equimolar mixture of ethanol and acetone, filling approximately two-thirds of the vial. The vial was then placed in a microwave and irradiated at 393 K for 2 minutes. Following the addition of acetone, colourless crystals of **(I)** were obtained after 15 days at room temperature. Yield: 90%

## 7. Refinement

Crystal data, data collection and structure refinement details are summarized in Table 2. Hydrogen atoms were positioned geometrically and allowed to ride on their parent atoms with C—H = 0.95–0.99 Å and O—H = 0.84 Å. The constraint  $U_{\text{iso}}(\text{H}) = 1.2U_{\text{eq}}(\text{C})$  or  $1.5U_{\text{eq}}(\text{methyl C or O})$  was applied in all cases.

**Table 2**  
Experimental details.

Crystal data	
Chemical formula	$\text{C}_{15}\text{H}_{12}\text{N}_2\text{O}_3$
$M_r$	268.27
Crystal system, space group	Monoclinic, $P2_1/c$
Temperature (K)	150
$a, b, c$ (Å)	11.2440 (19), 12.604 (2), 8.9926 (14)
$\beta$ (°)	106.870 (6)
$V$ (Å <sup>3</sup> )	1219.6 (3)
$Z$	4
Radiation type	Mo $K\alpha$
$\mu$ (mm <sup>-1</sup> )	0.10
Crystal size (mm)	0.25 × 0.2 × 0.18
Data collection	
Diffractometer	D8 VENTURE Bruker AXS
Absorption correction	Multi-scan (SADABS; Krause <i>et al.</i> , 2015)
No. of measured, independent and observed [ $I > 2\sigma(I)$ ] reflections	9853, 2781, 2205
$R_{\text{int}}$	0.046
$(\sin \theta/\lambda)_{\text{max}}$ (Å <sup>-1</sup> )	0.650
Refinement	
$R[F^2 > 2\sigma(F^2)], wR(F^2), S$	0.052, 0.132, 1.03
No. of reflections	2781
No. of parameters	183
H-atom treatment	H-atom parameters constrained
$\Delta\rho_{\text{max}}, \Delta\rho_{\text{min}}$ (e Å <sup>-3</sup> )	0.30, -0.28

Computer programs: APEX3 and SAINT (Bruker, 2015), SHELXT2018/2 (Sheldrick, 2015a), SHELXL2018/3 (Sheldrick, 2015b) and OLEX2 (Dolomanov *et al.*, 2009).

## Acknowledgements

We sincerely thank the OMC team at the University of Rennes, CNRS, Institut des Sciences Chimiques de Rennes (ISCR)–UMR 6226, France, for their valuable assistance during BT's internship and for their support of the data collection.

## Funding information

We gratefully acknowledge the financial support provided by the Ministry of Higher Education and Scientific Research of Algeria (MESRS) and the General Directorate for Scientific Research and Technological Development (DGRSDT).

## References

- Benlatreche, T. (2023). *CSD communication* (CCDC 2269924). CCDC, Cambridge, England.
- Bruker (2015). *APEX3* and *SAINT*. Bruker AXS Inc., Madison, Wisconsin, USA.
- Deegan, C., Coyle, B., McCann, M., Devereux, M. & Egan, D. A. (2006). *Chem. Biol. Interact.* **164**, 115–125.
- Dolomanov, O. V., Bourhis, L. J., Gildea, R. J., Howard, J. A. K. & Puschmann, H. (2009). *J. Appl. Cryst.* **42**, 339–341.
- Ermakova, E. A., Golubeva, J. A., Smirnova, K. S., Klyushova, L. S., Eltsov, I. V., Zubenko, A. A., Fetisov, L. N., Svyatogorova, A. E. & Lider, E. V. (2023). *Polyhedron* **230**, 116213.
- Fujihara, T., Wada, T. & Tanaka, K. (2004). *Dalton Trans.* pp. 645–652.
- Galdino, A. C. M., Viganor, L., Pereira, M. M., Devereux, M., McCann, M., Branquinha, M. H., Molphy, Z., O'Carroll, S., Bain, C., Menounou, G., Kellett, A. & dos Santos, A. L. S. (2022). *J. Biol. Inorg. Chem.* **27**, 201–213.
- Golubeva, Yu. A., Smirnova, K. S., Klyushova, L. S., Berezin, A. S. & Lider, E. V. (2023). *Russ. J. Coord. Chem.* **49**, 528–541.
- Granato, M. Q., Gonçalves, D. S., Seabra, S. H., McCann, M., Devereux, M., dos Santos, A. L. S. & Kneipp, L. F. (2017). *Front. Microbiol.* **8**, 76.
- Granato, M. Q., Mello, T. P., Nascimento, R. S., Pereira, M. D., Rosa, T. L. S. A., Pessolani, M. C. V., McCann, M., Devereux, M., Branquinha, M. H., Santos, A. L. S. & Kneipp, L. F. (2021). *Front. Microbiol.* **12**, 641258.
- Groom, C. R., Bruno, I. J., Lightfoot, M. P. & Ward, S. C. (2016). *Acta Cryst.* **B72**, 171–179.
- Jing, X., Zhu, Y.-L., Ma, K.-R., Cao, L. & Shao, S. (2011). *Acta Cryst.* **E67**, m957–m958.
- Karnahl, M., Tschierlei, S., Kuhnt, C., Dietzek, B., Schmitt, M., Popp, J., Schwalbe, M., Kriek, S., Görls, H., Heinemann, F. & Rau, S. (2010). *Dalton Trans.* **39**, 2359–2366.
- Krause, L., Herbst-Irmer, R., Sheldrick, G. M. & Stalke, D. (2015). *J. Appl. Cryst.* **48**, 3–10.
- McCann, M., Santos, A. L. S., da Silva, B. A., Romanos, M. T. V., Pyrrho, A. S., Devereux, M., Kavanagh, K., Fichtner, I. & Kellett, A. (2012). *Toxicology Research* **1**, 47–54.
- Pivetta, T., Trudu, F., Valletta, E., Isaia, F., Castellano, C., Demartin, F., Tuveri, R., Vascellari, S. & Pani, A. (2014). *J. Inorg. Biochem.* **141**, 103–113.
- Sheldrick, G. M. (2015a). *Acta Cryst.* **A71**, 3–8.
- Sheldrick, G. M. (2015b). *Acta Cryst.* **C71**, 3–8.
- Spackman, P. R., Turner, M. J., McKinnon, J. J., Wolff, S. K., Grimwood, D. J., Jayatilaka, D. & Spackman, M. A. (2021). *J. Appl. Cryst.* **54**, 1006–1011.

## supporting information

*Acta Cryst.* (2026). E82 [https://doi.org/10.1107/S2056989026004408]

## Synthesis and structure of (*RS*)-6-hydroxy-6-(2-oxopropyl)-1,10-phenanthroline-5(*6H*)-one

Tarek Benlatreche, Abderrahmane Mezrag, Boutheina Boualia and Stéphane Golhen

### Computing details

#### (*RS*)-6-Hydroxy-6-(2-oxopropyl)-1,10-phenanthroline-5(*6H*)-one

##### Crystal data

C<sub>15</sub>H<sub>12</sub>N<sub>2</sub>O<sub>3</sub>

*M<sub>r</sub>* = 268.27

Monoclinic, *P*2<sub>1</sub>/*c*

*a* = 11.2440 (19) Å

*b* = 12.604 (2) Å

*c* = 8.9926 (14) Å

β = 106.870 (6)°

*V* = 1219.6 (3) Å<sup>3</sup>

*Z* = 4

*F*(000) = 560

*D<sub>x</sub>* = 1.461 Mg m<sup>-3</sup>

Mo *K*α radiation, λ = 0.71073 Å

Cell parameters from 6286 reflections

θ = 2.5–27.5°

μ = 0.10 mm<sup>-1</sup>

*T* = 150 K

Prism, colourless

0.25 × 0.2 × 0.18 mm

##### Data collection

D8 VENTURE Bruker AXS  
diffractometer

Detector resolution: 10.4167 pixels mm<sup>-1</sup>  
rotation images scans

Absorption correction: multi-scan  
(SADABS; Krause *et al.*, 2015)

2781 independent reflections

2205 reflections with *I* > 2σ(*I*)

*R*<sub>int</sub> = 0.046

θ<sub>max</sub> = 27.5°, θ<sub>min</sub> = 2.5°

*h* = -14→14

*k* = -13→16

*l* = -11→11

9853 measured reflections

##### Refinement

Refinement on *F*<sup>2</sup>

Least-squares matrix: full

*R*[*F*<sup>2</sup> > 2σ(*F*<sup>2</sup>)] = 0.052

*wR*(*F*<sup>2</sup>) = 0.132

*S* = 1.03

2781 reflections

183 parameters

0 restraints

Primary atom site location: dual

Hydrogen site location: inferred from  
neighbouring sites

H-atom parameters constrained

*w* = 1/[σ<sup>2</sup>(*F*<sub>o</sub><sup>2</sup>) + (0.0414*P*)<sup>2</sup> + 1.046*P*]

where *P* = (*F*<sub>o</sub><sup>2</sup> + 2*F*<sub>c</sub><sup>2</sup>)/3

(Δ/σ)<sub>max</sub> < 0.001

Δρ<sub>max</sub> = 0.30 e Å<sup>-3</sup>

Δρ<sub>min</sub> = -0.28 e Å<sup>-3</sup>

##### Special details

**Geometry.** All esds (except the esd in the dihedral angle between two l.s. planes) are estimated using the full covariance matrix. The cell esds are taken into account individually in the estimation of esds in distances, angles and torsion angles; correlations between esds in cell parameters are only used when they are defined by crystal symmetry. An approximate (isotropic) treatment of cell esds is used for estimating esds involving l.s. planes.

Fractional atomic coordinates and isotropic or equivalent isotropic displacement parameters ( $\text{\AA}^2$ )

	<i>x</i>	<i>y</i>	<i>z</i>	$U_{\text{iso}}^*/U_{\text{eq}}$
O1	0.66938 (12)	0.29055 (10)	0.12038 (15)	0.0220 (3)
H1	0.606402	0.305120	0.046242	0.033*
O3	0.84247 (13)	0.52378 (11)	0.43924 (16)	0.0299 (3)
O2	0.88727 (13)	0.39743 (12)	0.10860 (18)	0.0333 (4)
N1	0.47777 (13)	0.60754 (12)	0.17416 (17)	0.0194 (3)
N2	0.63092 (14)	0.70543 (12)	0.03798 (17)	0.0208 (3)
C12	0.57858 (15)	0.55159 (14)	0.16619 (18)	0.0152 (3)
C11	0.66176 (15)	0.60569 (14)	0.08928 (18)	0.0165 (4)
C7	0.76747 (15)	0.55389 (15)	0.07228 (19)	0.0183 (4)
C4	0.60379 (15)	0.44875 (14)	0.22495 (19)	0.0161 (4)
C3	0.52129 (16)	0.40246 (15)	0.29597 (19)	0.0194 (4)
H3	0.533697	0.331769	0.333955	0.023*
C5	0.71304 (16)	0.38418 (14)	0.20787 (19)	0.0174 (4)
C6	0.79761 (16)	0.44393 (15)	0.1278 (2)	0.0200 (4)
C10	0.70589 (18)	0.75471 (15)	-0.0311 (2)	0.0242 (4)
H10	0.685095	0.824996	-0.067532	0.029*
C14	0.84877 (15)	0.43219 (16)	0.4815 (2)	0.0215 (4)
C8	0.84341 (16)	0.60787 (16)	-0.0011 (2)	0.0226 (4)
H8	0.915370	0.574755	-0.014840	0.027*
C13	0.79505 (16)	0.34433 (15)	0.3669 (2)	0.0206 (4)
H13A	0.744812	0.296932	0.412625	0.025*
H13B	0.864221	0.301854	0.350456	0.025*
C1	0.40297 (17)	0.56254 (16)	0.2471 (2)	0.0226 (4)
H1A	0.333471	0.601967	0.256368	0.027*
C2	0.42114 (16)	0.46134 (16)	0.3101 (2)	0.0214 (4)
H2	0.365825	0.432869	0.362005	0.026*
C9	0.81238 (18)	0.70962 (17)	-0.0529 (2)	0.0267 (4)
H9	0.862611	0.748262	-0.102620	0.032*
C15	0.90883 (18)	0.39957 (18)	0.6461 (2)	0.0291 (5)
H15A	0.988278	0.364693	0.653789	0.044*
H15B	0.854171	0.350215	0.679350	0.044*
H15C	0.923377	0.462428	0.713143	0.044*

Atomic displacement parameters ( $\text{\AA}^2$ )

	$U^{11}$	$U^{22}$	$U^{33}$	$U^{12}$	$U^{13}$	$U^{23}$
O1	0.0252 (7)	0.0134 (7)	0.0246 (7)	0.0021 (5)	0.0030 (5)	-0.0026 (5)
O3	0.0307 (7)	0.0206 (8)	0.0337 (7)	-0.0007 (6)	0.0021 (6)	0.0004 (6)
O2	0.0312 (7)	0.0280 (8)	0.0482 (9)	0.0095 (6)	0.0234 (7)	0.0086 (7)
N1	0.0195 (7)	0.0160 (8)	0.0235 (7)	0.0012 (6)	0.0072 (6)	-0.0008 (6)
N2	0.0263 (8)	0.0150 (8)	0.0210 (7)	0.0009 (6)	0.0065 (6)	0.0020 (6)
C12	0.0169 (8)	0.0147 (9)	0.0137 (7)	-0.0003 (6)	0.0041 (6)	-0.0020 (6)
C11	0.0185 (8)	0.0148 (9)	0.0148 (7)	-0.0011 (6)	0.0025 (6)	-0.0010 (6)
C7	0.0177 (8)	0.0192 (9)	0.0171 (8)	-0.0017 (7)	0.0035 (6)	-0.0003 (7)
C4	0.0182 (8)	0.0149 (9)	0.0146 (7)	-0.0001 (6)	0.0037 (6)	-0.0026 (6)

C3	0.0240 (9)	0.0153 (9)	0.0186 (8)	-0.0017 (7)	0.0058 (7)	0.0016 (7)
C5	0.0211 (8)	0.0116 (8)	0.0195 (8)	0.0013 (7)	0.0060 (6)	0.0026 (7)
C6	0.0200 (8)	0.0192 (10)	0.0213 (8)	0.0030 (7)	0.0068 (7)	0.0009 (7)
C10	0.0308 (10)	0.0162 (10)	0.0252 (9)	-0.0020 (8)	0.0073 (7)	0.0047 (7)
C14	0.0157 (8)	0.0257 (11)	0.0233 (9)	0.0027 (7)	0.0062 (7)	0.0025 (8)
C8	0.0195 (8)	0.0246 (10)	0.0242 (9)	-0.0007 (7)	0.0071 (7)	0.0019 (8)
C13	0.0224 (8)	0.0183 (10)	0.0195 (8)	0.0036 (7)	0.0038 (7)	0.0026 (7)
C1	0.0202 (8)	0.0229 (10)	0.0263 (9)	0.0013 (7)	0.0091 (7)	-0.0035 (8)
C2	0.0222 (9)	0.0239 (10)	0.0203 (8)	-0.0034 (7)	0.0098 (7)	-0.0013 (7)
C9	0.0265 (9)	0.0280 (11)	0.0270 (9)	-0.0052 (8)	0.0101 (7)	0.0061 (8)
C15	0.0252 (9)	0.0380 (13)	0.0223 (9)	-0.0042 (9)	0.0040 (7)	0.0019 (9)

*Geometric parameters (Å, °)*

O1—H1	0.8400	C5—C6	1.545 (2)
O1—C5	1.424 (2)	C5—C13	1.543 (2)
O3—C14	1.211 (2)	C10—H10	0.9500
O2—C6	1.221 (2)	C10—C9	1.390 (3)
N1—C12	1.354 (2)	C14—C13	1.514 (3)
N1—C1	1.334 (2)	C14—C15	1.496 (2)
N2—C11	1.349 (2)	C8—H8	0.9500
N2—C10	1.336 (2)	C8—C9	1.375 (3)
C12—C11	1.481 (2)	C13—H13A	0.9900
C12—C4	1.398 (2)	C13—H13B	0.9900
C11—C7	1.403 (2)	C1—H1A	0.9500
C7—C6	1.479 (3)	C1—C2	1.386 (3)
C7—C8	1.398 (2)	C2—H2	0.9500
C4—C3	1.397 (2)	C9—H9	0.9500
C4—C5	1.518 (2)	C15—H15A	0.9800
C3—H3	0.9500	C15—H15B	0.9800
C3—C2	1.385 (3)	C15—H15C	0.9800
C5—O1—H1	109.5	C9—C10—H10	117.9
C1—N1—C12	117.48 (16)	O3—C14—C13	120.55 (16)
C10—N2—C11	117.24 (16)	O3—C14—C15	122.76 (18)
N1—C12—C11	115.89 (15)	C15—C14—C13	116.69 (17)
N1—C12—C4	122.95 (15)	C7—C8—H8	120.5
C4—C12—C11	121.15 (15)	C9—C8—C7	118.99 (17)
N2—C11—C12	117.01 (15)	C9—C8—H8	120.5
N2—C11—C7	122.56 (16)	C5—C13—H13A	108.8
C7—C11—C12	120.43 (16)	C5—C13—H13B	108.8
C11—C7—C6	121.18 (15)	C14—C13—C5	113.94 (15)
C8—C7—C11	118.54 (17)	C14—C13—H13A	108.8
C8—C7—C6	120.28 (16)	C14—C13—H13B	108.8
C12—C4—C5	122.71 (15)	H13A—C13—H13B	107.7
C3—C4—C12	118.12 (16)	N1—C1—H1A	118.2
C3—C4—C5	119.11 (16)	N1—C1—C2	123.56 (17)
C4—C3—H3	120.5	C2—C1—H1A	118.2

C2—C3—C4	118.91 (17)	C3—C2—C1	118.88 (16)
C2—C3—H3	120.5	C3—C2—H2	120.6
O1—C5—C4	109.93 (14)	C1—C2—H2	120.6
O1—C5—C6	107.86 (14)	C10—C9—H9	120.7
O1—C5—C13	105.05 (14)	C8—C9—C10	118.54 (17)
C4—C5—C6	114.29 (14)	C8—C9—H9	120.7
C4—C5—C13	111.36 (14)	C14—C15—H15A	109.5
C13—C5—C6	107.89 (14)	C14—C15—H15B	109.5
O2—C6—C7	121.31 (16)	C14—C15—H15C	109.5
O2—C6—C5	118.50 (16)	H15A—C15—H15B	109.5
C7—C6—C5	120.17 (15)	H15A—C15—H15C	109.5
N2—C10—H10	117.9	H15B—C15—H15C	109.5
N2—C10—C9	124.13 (18)		
O1—C5—C6—O2	-57.0 (2)	C11—C7—C8—C9	0.4 (3)
O1—C5—C6—C7	121.28 (16)	C7—C8—C9—C10	-0.4 (3)
O1—C5—C13—C14	-178.29 (14)	C4—C12—C11—N2	-179.14 (15)
O3—C14—C13—C5	-11.3 (2)	C4—C12—C11—C7	0.7 (2)
N1—C12—C11—N2	1.4 (2)	C4—C3—C2—C1	2.8 (3)
N1—C12—C11—C7	-178.76 (14)	C4—C5—C6—O2	-179.53 (16)
N1—C12—C4—C3	-0.5 (2)	C4—C5—C6—C7	-1.3 (2)
N1—C12—C4—C5	176.56 (15)	C4—C5—C13—C14	-59.34 (19)
N1—C1—C2—C3	-0.7 (3)	C3—C4—C5—O1	58.65 (19)
N2—C11—C7—C6	-179.12 (15)	C3—C4—C5—C6	-179.92 (14)
N2—C11—C7—C8	-0.2 (3)	C3—C4—C5—C13	-57.3 (2)
N2—C10—C9—C8	0.1 (3)	C5—C4—C3—C2	-179.43 (15)
C12—N1—C1—C2	-2.0 (3)	C6—C7—C8—C9	179.34 (16)
C12—C11—C7—C6	1.0 (2)	C6—C5—C13—C14	66.84 (18)
C12—C11—C7—C8	179.99 (15)	C10—N2—C11—C12	179.80 (15)
C12—C4—C3—C2	-2.3 (2)	C10—N2—C11—C7	-0.1 (2)
C12—C4—C5—O1	-118.38 (16)	C8—C7—C6—O2	-1.4 (3)
C12—C4—C5—C6	3.1 (2)	C8—C7—C6—C5	-179.59 (16)
C12—C4—C5—C13	125.62 (17)	C13—C5—C6—O2	56.0 (2)
C11—N2—C10—C9	0.1 (3)	C13—C5—C6—C7	-125.72 (16)
C11—C12—C4—C3	-179.94 (15)	C1—N1—C12—C11	-177.91 (15)
C11—C12—C4—C5	-2.9 (2)	C1—N1—C12—C4	2.6 (2)
C11—C7—C6—O2	177.55 (17)	C15—C14—C13—C5	168.82 (15)
C11—C7—C6—C5	-0.7 (2)		

Hydrogen-bond geometry ( $\text{\AA}$ ,  $^\circ$ )

$D-H\cdots A$	$D-H$	$H\cdots A$	$D\cdots A$	$D-H\cdots A$
O1—H1 $\cdots$ N1 <sup>i</sup>	0.84	2.22	2.977 (2)	149
O1—H1 $\cdots$ N2 <sup>i</sup>	0.84	2.56	3.262 (2)	142
C13—H13A $\cdots$ O1 <sup>ii</sup>	0.99	2.52	3.457 (2)	158
C15—H15B $\cdots$ O1 <sup>ii</sup>	0.98	2.67	3.561 (3)	152
C1—H1A $\cdots$ O1 <sup>iii</sup>	0.95	2.63	3.302 (2)	128
C3—H3 $\cdots$ N1 <sup>iii</sup>	0.95	2.83	3.727 (2)	158

---

C8—H8···O2 <sup>iv</sup>	0.95	2.62	3.436 (3)	145
C10—H10···O3 <sup>v</sup>	0.95	2.59	3.235 (2)	125
C15—H15A···O3 <sup>vi</sup>	0.98	2.69	3.254 (3)	117

---

Symmetry codes: (i)  $-x+1, -y+1, -z$ ; (ii)  $x, -y+1/2, z+1/2$ ; (iii)  $-x+1, y+1/2, -z+1/2$ ; (iv)  $-x+2, -y+1, -z$ ; (v)  $x, -y+3/2, z-1/2$ ; (vi)  $-x+2, -y+1, -z+1$ .